WESE

WAVE ENERGY
IN SOUTHERN EUROPE

DELIVERABLE 3.3
MARINE DYNAMICS MODELLING

This project has been funded by the European Commission under the European Maritime and Fisheries Fund (EMFF), Call for Proposals EASME/EMFF/2017/1.2.1.1 – "Environmental monitoring of wave and tidal devices". This communication reflects only the author's view. EASME is not responsible for any use that may be made of the information it contains.

AZTI MEMBER OF BASQUE RESEARCH & TECHNOLOGY ALLIANCE · WavEC Offshore Renewables · IDOM · BiMEP Biscay Marine Energy Platform · CTN · WAVEROLLER® by AW-Energy · HIDROMOD

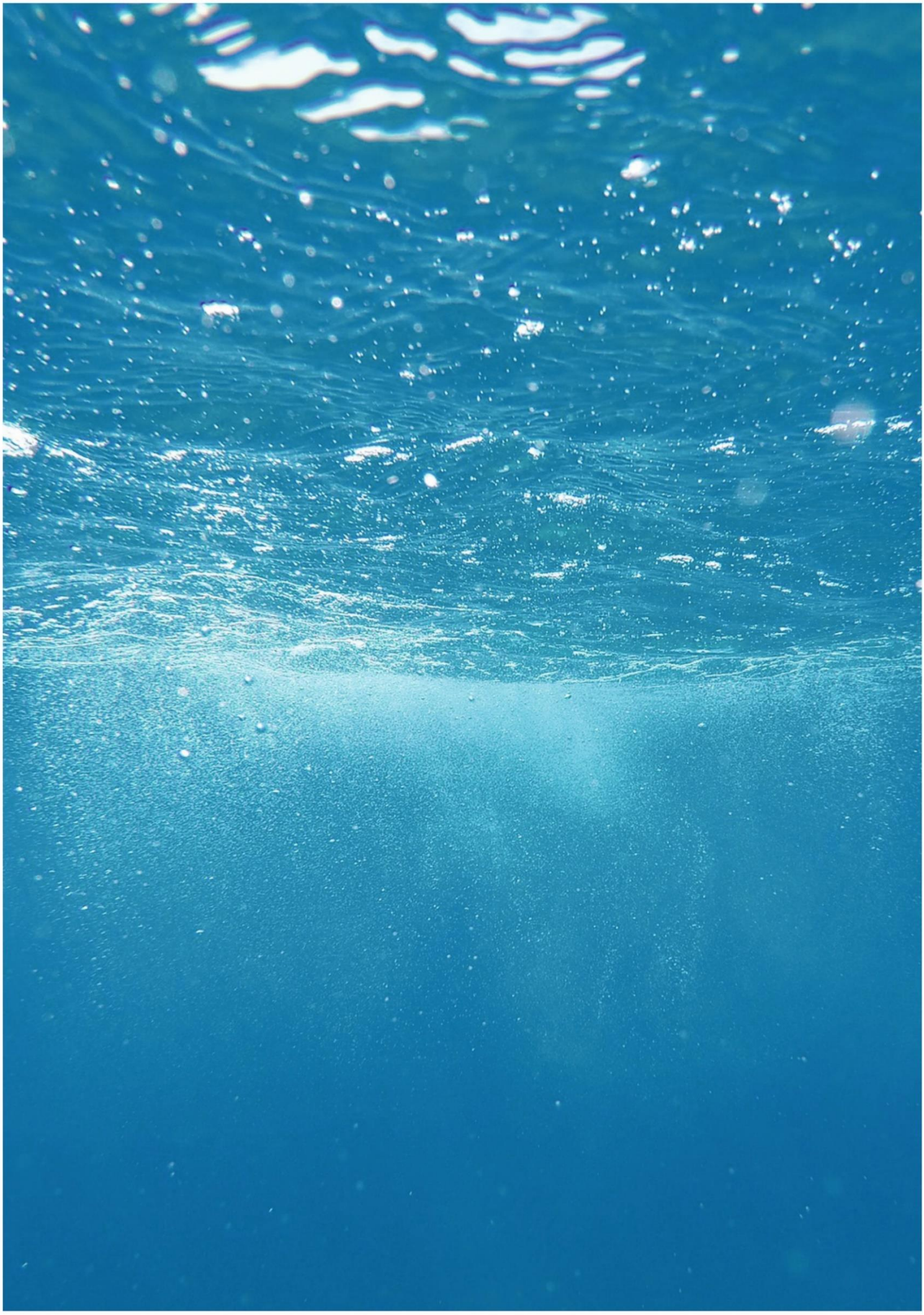

WP 3

Deliverable 3.3 Marine dynamics modelling

PROJECT COORDINATOR

AZTI

TASK LEADER

Iñaki de Santiago

AUTHORS

Iñaki de Santiago – AZTI
Theo Moura - HIDROMOD
José Chambel - HIDROMOD
Pedro Liria -AZTI
Juan Bald - AZTI

SUBMISSION DATE

14 | 05| 2021

CITATION

de Santiago, I., Moura, T., Chambel, J., Liria, P., and Bald, J., 2020. Deliverable 3.3 Marine dynamics modelling. Deliverable of the WESE Project funded by the European Commission. Agreement number EASME/EMFF/2017/1.2.1.1/02/SI2.787640. 37 pp.

This project has been funded by the European Commission under the European Maritime and Fisheries Fund (EMFF), Call for Proposals EASME/EMFF/2017/1.2.1.1 – "Environmental monitoring of wave and tidal devices". This communication reflects only the author's view. EASME is not responsible for any use that may be made of the information it contains.

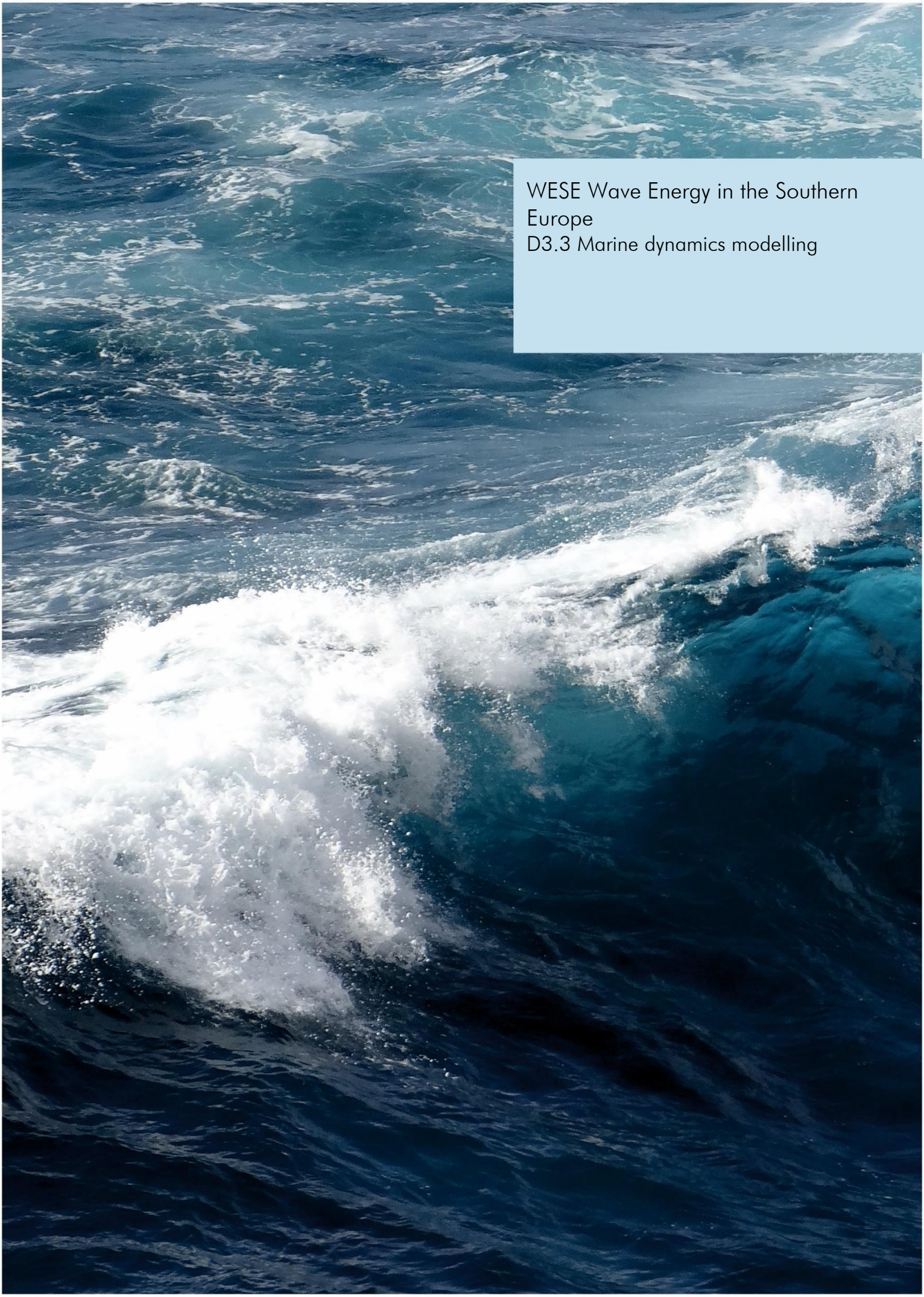

WESE Wave Energy in the Southern Europe

D3.3 Marine dynamics modelling

CONTENTS

List of Figures

1. WESE project synopsis

The Atlantic seaboard offers a vast marine renewable energy (MRE) resource which is still far from being exploited. These resources include offshore wind, wave and tidal. This industrial activity holds considerable potential for enhancing the diversity of energy sources, reducing greenhouse gas emissions, and stimulating and diversifying the economies of coastal communities. Therefore, the ocean energy development is one of the main pillars of the EU Blue Growth strategy. While the technological development of devices is growing fast, their potential environmental effects are not well-known. In a new industry like MRE, and Wave Energy (WE) in particular, there may be interactions between devices and marine organisms or habitats that regulators or stakeholders perceive as risky. In many instances, this perception of risk is due to the high degree of uncertainty that results from a paucity of data collected in the ocean. However, the possibility of real risk to marine organisms or habitats cannot be ignored; the lack of data continues to confound our ability to differentiate between real and perceived risks. Due to the present and future demand for marine resources and space, human activities in the marine environment are expected to increase, which will produce higher pressures on marine ecosystems, as well as competition and conflicts among marine users. This context still continues to present challenges to permitting/consenting of commercial-scale development. Time-consuming procedures linked to uncertainty about project environmental impacts, the need to consult with numerous stakeholders and potential conflicts with other marine users appear to be the main obstacles to consenting WE projects. These are considered as non-technological barriers that could hinder the future development of WE in EU and Spain and Portugal in particular were, for instance, consenting approaches remain fragmented and sequential. Consequently, and in accordance with the Ocean Energy Strategic Roadmap published in November 20161, the main aim of the project consists on overcoming these non-technological barriers through the following specific objectives:

- Development of environmental monitoring around wave energy converters (WECs) operating at sea, to analyse, share and improve the knowledge of the positive and negative environmental pressures and impacts of these technologies and consequently a better knowledge of real risks.
- The resulting data collection will be used to apply and improve existing modelling tools and contribute to the overall understanding of potential cumulative pressures and impacts of larger scale, and future, wave energy deployments.

- Development of efficient guidance for planning and consenting procedures in Spain and Portugal for WE projects, to better inform decision-makers and managers on environmental real risks and reduce environmental consenting uncertainty of ocean WE introducing the Risk Based Approach suggested by the RiCORE, a Horizon 2020 project, which underline the difficulties for developers with an existing fragmented and sequential consenting approaches in these countries;
- Development and implementation of innovative maritime spatial planning (MSP) Decision Support Tools (DSTs) for Portugal and Spain for site selection of WE projects. The final objective of such tools will be the identification and selection of suitable areas for WE development, as well as to support decision makers and developers during the licensing process. These DSTs will consider previous findings (both environmental and legal, found in RiCORE) and the new knowledge acquired in WESE in order to support the development of the risk-based approach mentioned in iii);
- Development of a Data Sharing Platform that will serve data providers, developers and regulators. This includes the partners of the project. WESE Data Platform will be made of a number of ICT services in order to have: (i) a single web access point to relevant data (either produced within the project or by others); (ii) Generation of OGC compliant requests to access data via command line (advanced users); (iii) a dedicated cloud server to store frequently used data or data that may not fit in existing Data Portals; (iv) synchronized biological data and environmental parameters in order to feed models automatically.

2. Executive summary

The need of slowing down the global temperature increase due to climate change, has resulted in the search of new strategies to capture energy with low greenhouse gas emissions. In this line, ocean energy can both contribute to the reduction of greenhouse gas emissions and foster economic growth in coastal areas (Magagna and Uihlein, 2015).

While the technological development of devices is growing fast, their effects on coastal environments are not well-known and therefore these must be thoroughly investigated prior to WEC implementation. For that, new and modified versions of wave propagation models that allow the incorporation of device-specific WEC characteristics to specify obstacle transmission were developed and tested recently (Chang et al., 2016; McNatt et al., 2020; Millar et al., 2007). Several studies were carried out to assess WEC farms driven nearshore hydrodynamic impacts. Previous studies show that while the reduction of the significant wave height in the lee of the WEC farm can be relevant (up to 30%) it might be considerably variable depending on the WEC technology, distance from the WEC farm to the coast, initial wave conditions, and the configurations of WEC farm (Atan et al., 2019; Carballo and Iglesias, 2013; Chang et al., 2016; Contardo et al., 2018; Rusu and Soares, 2013). On the other hand, some relevant conclusions were drawn so far regarding the impact of WEC farm on beaches. For example, the discovery of the added benefit of the WEC farm by the possible substantial reduction in the beach erosion (Abanades et al., 2015; J Abanades et al., 2014a, 2014b; Bergillos et al., 2019a; Mendoza et al., 2014; Millar et al., 2007; Zanopol et al., 2014; Zanuttigh and Angelelli, 2013), coastal flooding (Bergillos et al., 2019a) and sea level rise driven shoreline erosion mitigation (Bergillos et al., 2019b).

An important aspect of WECs is the energy absorption dependency on wave frequency (for some devices also in wave amplitude), which varies according to their design. This dependency is expressed in terms of the Relative Capture Width curve (RCW) where the effective energy conversion is discretized in wave frequency, or the Power Matrix where the discretization is done both in frequency and amplitude.

Here, two case studies related to the impact of WECs on coastal morphodynamics are presented. The first case has the objective of investigating the long-term impacts of a WEC farm composed by a series of point absorber OWC (Oscillating Water Column) devices on nearshore wave climate and the consequences on the shoreline response; and the second case is focused on evaluating the changes in the wave spectrum

caused by the frequency dependent' energy absorption of bottom mounted energy converters and their impacts in the short-term morphological evolution.

3. MARMOK

3.1 Methodology

The understanding of the interactions between the WEC farm with the local wave climate is fundamental to investigate the effects of WEC farm on the coast. In this study this is done following a two-step approach: First, a baseline test excluding the WEC farm is conducted, and then the same test including the WEC farm is replicated. Finally, to evaluate the changes produced by the WEC farm, the baseline scenario is compared with the WEC farm scenario.

Here we focus on investigating WEC farm effects on coastal hydrodynamics and coastal morphodynamics.

3.1.1 WEC farm characteristics

One of the most relevant factors when performing a WEC farm impact analysis is the type of WEC that is being utilized, the number of devices deployed and the location where the WEC farm is set up. In the present case, a WEC farm composed by a series of MARMOK point absorber OWC (Oscillating Water Column) devices, developed during the European project OPERA (http://opera-h2020.eu/), is studied. The device is tied to the seabed with a mooring system based on anchors and it has a 15m diameter. In the present study, 80 WEC devices are located at 60-80 m water depth (4 km from the coast approx.) in the maritime testing site of Bimep, in the Bay of Biscay (Figure 1).

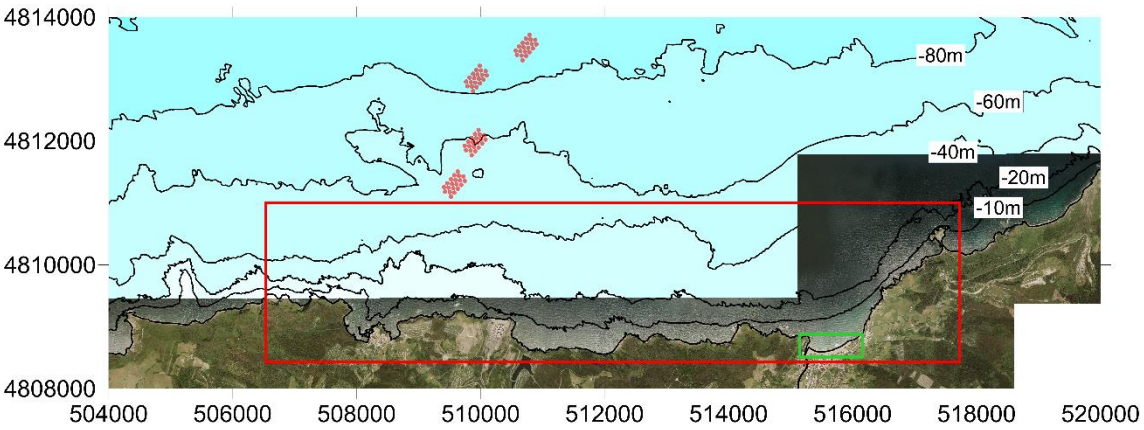

Figure 1. WEC farm location (BIMEP area, North of Spain). Red dots: WEC devices. Red box: Nearshore area under study. Green box: Bakio beach.

3.1.2 Wave modelling

For the wave propagation the SNL-SWAN is utilized (Chang et al., 2016). The model was specifically designed to evaluate the WEC farm effects on wave propagation. The model incorporates a WEC module that internally calculates the transmission coefficients based on the WEC power performance.

In order to propagate the deep water wave climate of the Bay of Biscay to the BIMEP coastal region, the wave data collected from the Downscaling Ocean Waves (DOW) database (Camus et al., 2013) at deep water propagated. The dataset is composed by 61 years of hourly spaced wave series. The transformation process (wave climate transference to coastal areas) is performed by combining dynamic and statistical downscaling as proposed by Camus et al., 2011. For that, a three-step approach iare used:

1. The maximum dissimilarity selection algorithm (MDA) is applied to obtain a representative sea state dataset. In the present case, 350 sea states were selected (Figure 2).
2. Each sea state is propagated to the coastal area. In the present study, 700 cases were propagated. 350 sea states without the presence of the WEC farm (baseline scenario) and 350 sea states in the presence of the WEC farm.
3. Once the sea states are propagated to the coast, the wave parameters (wave height, wave period, wave direction) are reconstructed using a non-linear interpolation technique based on radial basis functions (RBFs), at 200 locations 50m spaced along the nearshore are under study (red box in Figure 1).

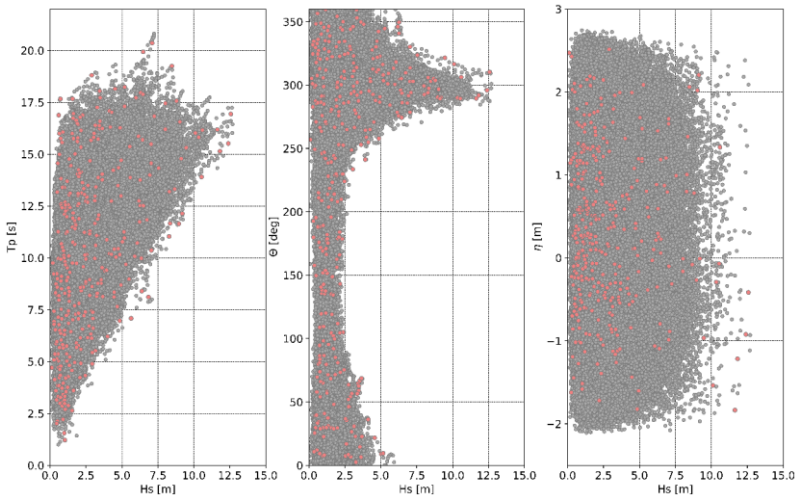

Figure 2. Wave climate parameters distribution at the Bilbao buoy (lat=43.64° lon=-3.09°). Grey dots: all sea states of DOW dataset at the Bilbao buoy. Red dots: Selected cases for wave propagation using the MDA algorithm.

3.1.3 Beach shoreline evolution modelling

3.1.3.1 *Shoreline evolution model*

The model used in the present work to analyse the shoreline response, takes into the longshore sediment transport due to waves and the cross-shore sediment transport due to water level variations produced by waves, tides and storm surges. The governing equation includes an alongshore transport one-line model that accounts for the influence of waves reaching the coast with a certain incident angle (first term on the right-hand side of equation eq. 1) and a cross-shore equilibrium shoreline model, which accounts for the effect of the wave action and the presence of varying water levels (second term on the right-hand side of eq. 1).

$$\frac{\partial y_s}{\partial t} = \frac{1}{h_c}\frac{\partial Q_l}{\partial x} + k_{ce,ca}\left(y_{s,eq} - y_s\right) \qquad \text{eq. 1}$$

The *ys* represents the position of the shoreline (here defined by the mean high water level MHW), *t* is time; *Ql* is the longshore sediment transport rate, *x* is the alongshore coordinate, *hc* is the closure depth (here estimated by Birkemeier, 1985), $y_{s,eq}$ represents the cross-shore equilibrium position and $k_{ce,ca}$ is an erosion/accretion rate control parameter.

3.1.3.2 *Shoreline evolution modelling strategy*

Long and short time scale shoreline variations are driven by different time scale events (e.g., long winter periods or short episodic storms). However, shoreline modulations not only depend on the hydrodynamic characteristics but also on how the shoreline position is located with respect to its equilibrium position. Because of that, how short and long-time scale wave sequences are distributed in time is relevant to correctly simulate the shoreline variations. Here a statistical model that can take the time-dependency of the integrated wave parameters into account is applied. It allows to generate a series of synthetic wave series and hence adequately model realistic shoreline dynamics considering the uncertainties involved. Here, 100 long-term synthetic multivariate hourly time series of significant wave height (Hs), wave peak period (Tp), wave peak direction (Dirw) and storm surge (ss) were generated. For that, a VAR (vector autoregression) model was fitted to the wave parameters (Hs, Tp, Dir)

and storm surge along the coast to model the time dependence and the inter-dependence of the multi-spatial conditions.

The methodology follows a three-step approach (Figure 3):

1. Original nearshore wave climate is collected from the desired locations (e.g., Bakio beach)
2. A MVAR model is fitted to the original wave climate
3. A synthetic nearshore wave climate is generated
4. The shoreline evolution model is applied with the nearshore synthetic wave climate as an input.
5. Redo step 3 to 4 as many times as necessary.

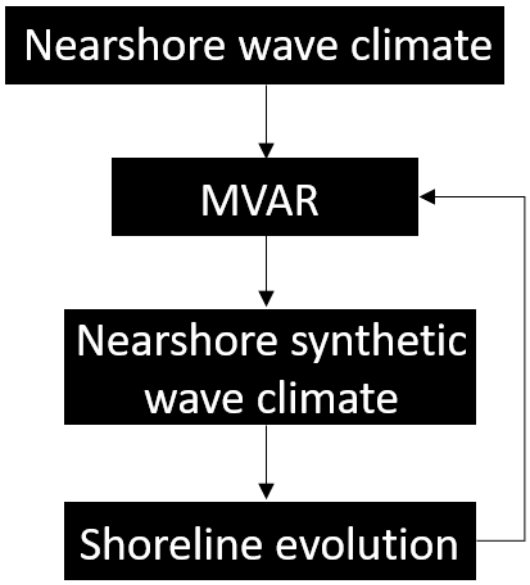

Figure 3. Scheme of the methodology to generate the synthetic wave series and shoreline evolution.

3.1.4 Nearshore impact indicators

3.1.4.1 *Hydrodynamic indicators*

The nearshore impact is characterized by evaluating the following indicators based on Iglesias and Carballo, 2014 study:

- Nearshore Impact (*NI*): Wave power and wave height difference between WEC farm scenario and baseline scenario at 20m depth contour.

$$\mathrm{NI} = \mathrm{P}_w^{20} - \mathrm{P}_b^{20} \qquad \text{eq. 2}$$

$$\mathrm{NI} = Hs_w^{20} - Hs_b^{20}$$

Where P_w^{20} (Hs_w^{20}) is the wave power (significant wave height) in the presence WEC farm at a generic point of the 20 m contour and P_b^{20} (Hs_b^{20}) is the wave power (significant wave height) without the presence of the WEC farm at a generic point of the 20 m.

- Maximum absolute Nearshore Impact (*NImax*): The maximum absolute value of NI.
- Maximum Nearshore Impact (*MNI*) location: Location where the maximum absolute value of NI occurs.
- Relative Nearshore Impact (*RNI*): The impact of the WEC farm on the nearshore wave power / significant wave height as a percentage of the baseline wave power / significant wave height.

$$\mathrm{RNI} = \frac{(\mathrm{P}_w^{20} - \mathrm{P}_b^{20})}{\mathrm{P}_b^{20}} \text{ x } 100 \qquad \text{eq. 3}$$

$$\mathrm{RNI} = \frac{(\mathrm{Hs}_w^{20} - Hs_b^{20})}{\mathrm{Hs}_b^{20}} \text{ x } 100$$

- Impact Extension (*IE*): The impact extension defined as the nearshore length where the RNI_{50} (RNI 50th percentile) is larger than 2.5%.

3.1.4.2 *Morphodynamic indicators*

- Shoreline location (*y*): Intersection between the dry part of the beach and the mean high-water level.
- Shoreline Impact (*SI*): Shoreline location difference between WEC farm scenario and baseline scenario.

3.2 Results

3.2.1 WEC farm impact on the nearshore wave conditions

The results of the indicators (*NI, NImax, MNI, RNI, IE*) are described in the following.

Figure 4 shows the *NI* in terms of P and Hs along the study area. The mean values (associated to the 50th percentile) vary in a range of -2000w/m - -4w/m and -0.06m – 0m, respectively, and present maximum reduction values (*NImax*) of 41443w/m and 0.45m (see Figure 5). It is observed that while the lowest NI are associated with P (Hs) values of around 100W/m (1m-3m) the lowest RNI are associated with lower values (Figure 6). On the other hand, due to the characteristics of the WEC, for sea states associated with P (Hs) greater than 400 W/m (5m), the reduction of energy is negligible because the WEC is deactivated for such sea states conditions.

The *NImax* point (red star in Figure 4) is located right at the south of the WEC farm, in front of a cliff area.

The reduction of P and Hs produced by the WEC farm can be defined as limited and practically with no effect at the coastline. This is mainly due to the distance at which the WEC farm is located from the coastal zone, which is far enough to significantly reduce the wave shadowing effect that occurs in the vicinity of the WEC farm.

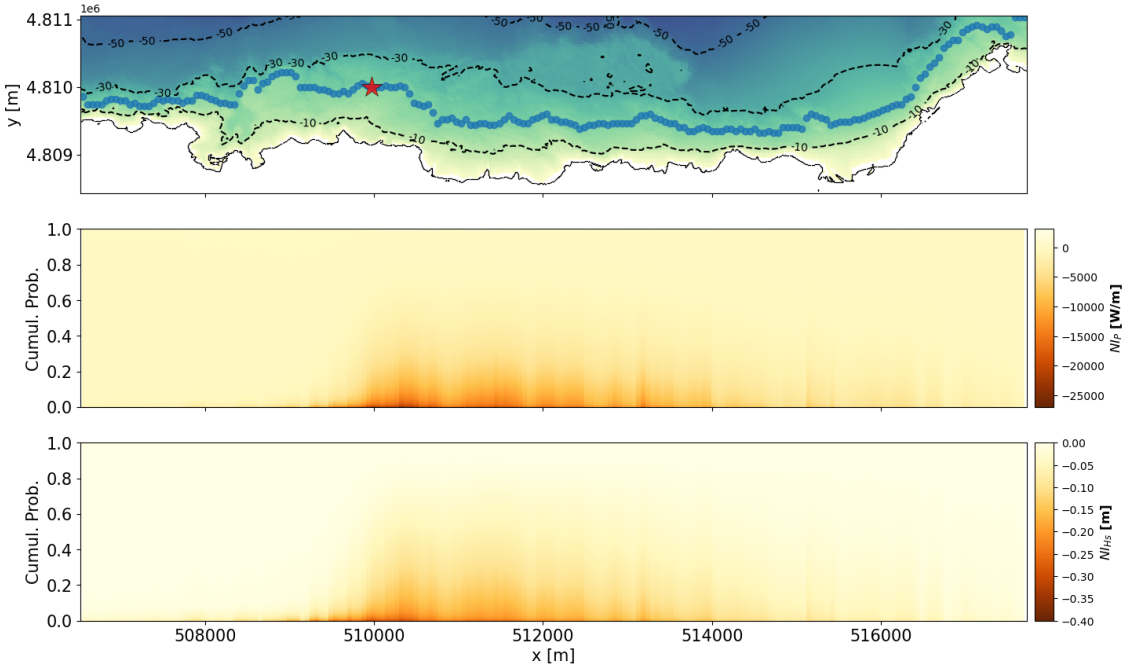

Figure 4. NI along the 20 m contour. Top: Nearshore area under study and analysed locations (blue dots). Red star indicates the MNI. Middle: RNI wave power. Bottom: RNI significant wave height.

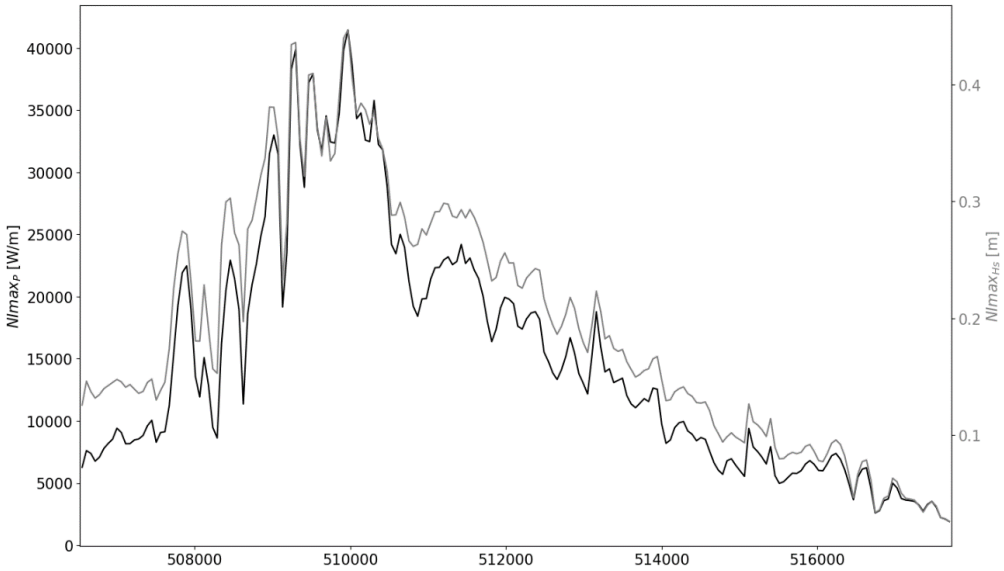

Figure 5. *NImax* along the 20 m contour.

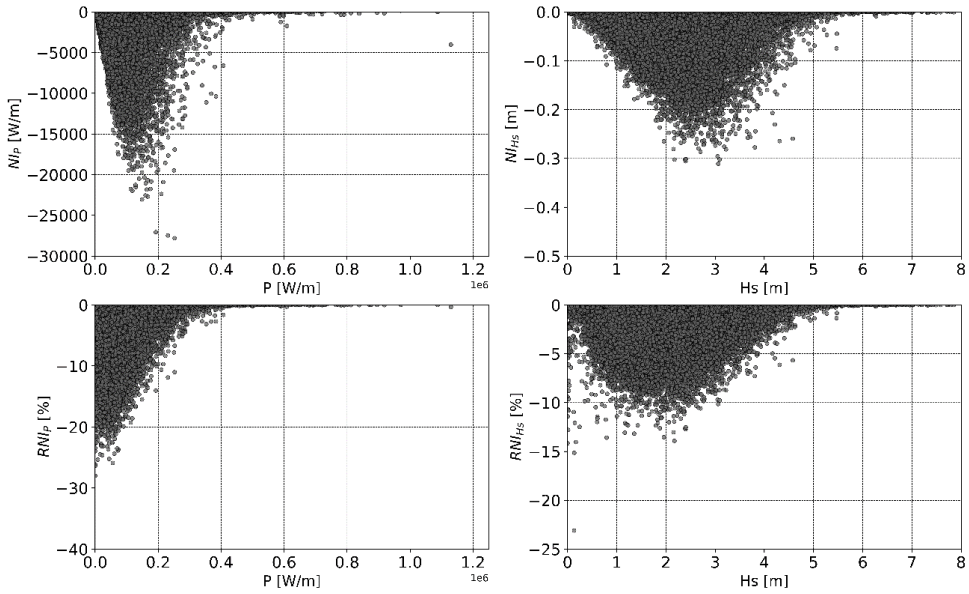

Figure 6. NI and RNI distribution based on $1 \cdot 10^5$ randomly selected cases.

The changes in P and Hs produced by the WEC farm in relative terms (*RNI*) are shown in Figure 7. The changes associated with the 50th percentile of the *RNI* ranges from -8% - 0% and -5% - 0% for P and Hs, respectively. Reductions of P and Hs greater than 10% are only recorded during 40% and 4% of the time, respectively. In other words, the 60% and 96% of the time, the buffering effect of the WEC farm on P and Hs is limited (P and Hs buffering greater than 10%).

On the other hand, the impact extension (*IE*) is of 5.5 km for P and 3 km for Hs and only covers rocky cliff areas where no human activities are carried out.

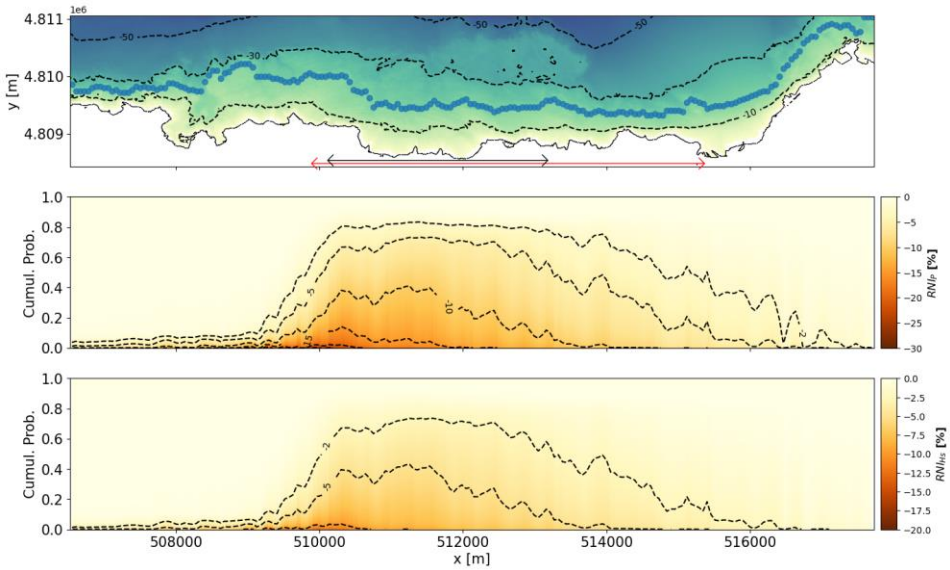

Figure 7. *RNI* along the 20 m contour. Top: Nearshore area under study and analysed locations (blue dots). Middle: RNI wave power. Bottom: RNI significant wave height. Red arrow: IE associated to P. Black arrow: IE associated to Hs.

3.2.2 Morphodynamic impact

The impact on beaches is quantified by the shoreline variability. The only beach within the study area is Bakio (green box in Figure 9a). The beach is located outside the *IE* region and presents a *NImax* of 7000w/m and 0.1m in terms of P and Hs, respectively. That is, the effect of the WEC farm on wave dynamics is minimal in this area.

Figure 8, shows the historical evolution of *y* in three different sectors of the beach (Figure 9a). Whether if the WEC farm is present or not, the number and the magnitude of erosion (negative values which are equivalent to a landward migration of the shoreline) and accretion (positive values which are equivalent to a seaward migration of the shoreline) events are similar in both scenarios.

The analysis of *SI* (Figure 9) is analysed using the 100 synthetic wave series obtained by means of MVAR method. The differences in *y* (50th percentile) between baseline and WEC farm scenarios are minimal (less than 3m). The *SI* is not homogeneous along the beach. While the western part of the beach undergoes a slight accretion (+2m), the central area is hardly modified and it is only on the eastern contour of the beach that there is a slight erosion area (-1.5m). However, it is worth highlighting that the range of differences between the baseline and WEC farm scenario is below the model's precision standards (5-10m). Therefore, although it can be assumed that the changes in the shoreline driven by the WEC farm are minimal, the magnitude of these differences should be taken as an approximate value, keeping in consideration the limitations of the shoreline evolution model.

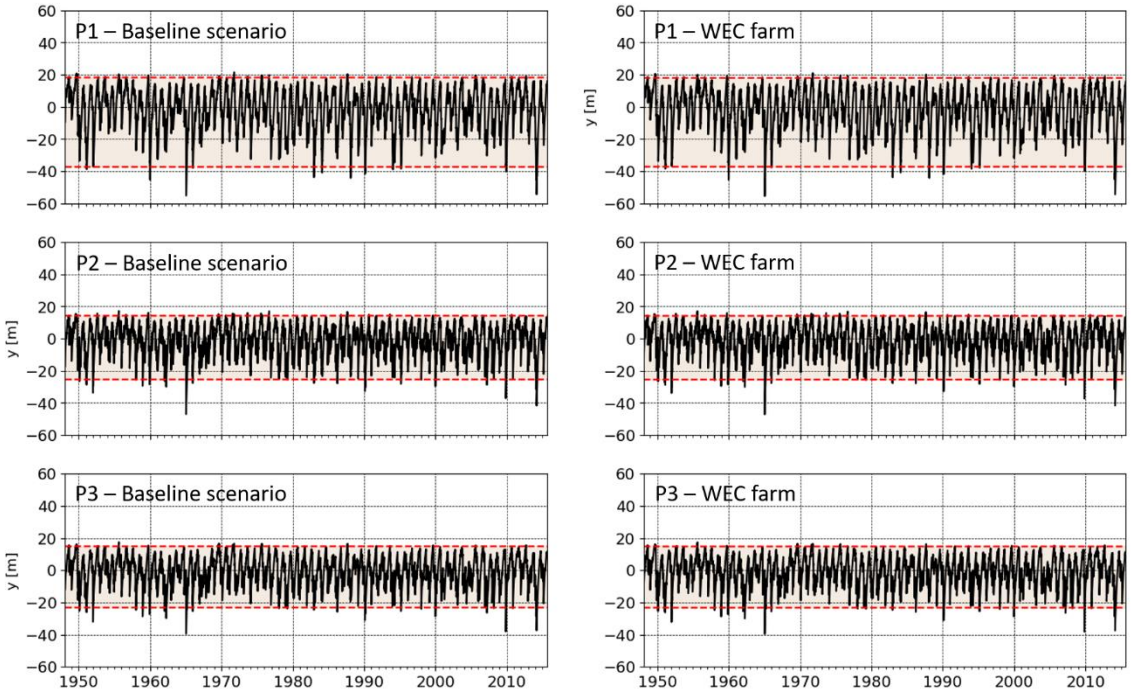

Figure 8. Historical shoreline position (*y*)variability in absence of WEC farm (baseline scenario) and in presence of WEC farm. Red shadow area: Area containing the 98% of the shoreline variability.

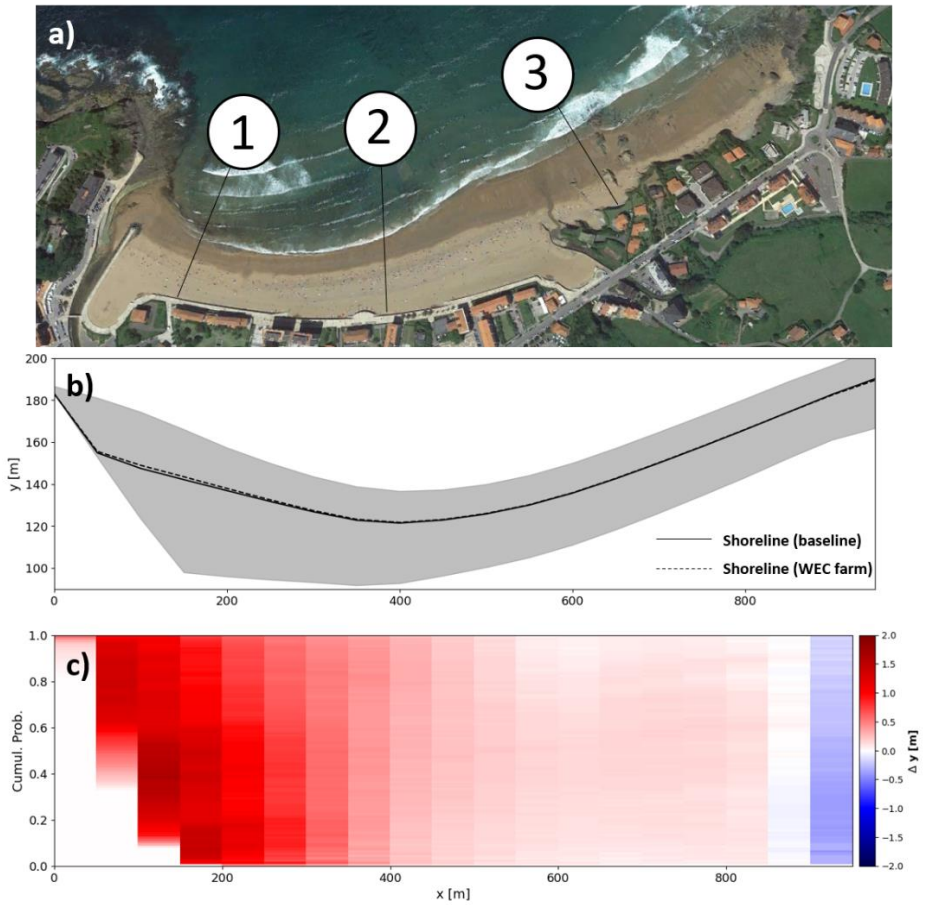

Figure 9. *SI* at Bakio beach. a) Bakio beach. b) Shoreline location (*y*) and accretion erosion limits (shadow zone). c) Spatial cumulative probability function of *SI*.

4. Waveroller

4.1 Methodology

4.1.1 Waveroller Specifications

The Waveroller is a bottom mounted energy converter. The device is 10 meter high with flopping panels that vary between 18 and 24 meters and are designed to be mounted at depths between 10 and 20 meters (Figure 10). The WEC array is designed to be two rows of devices with 50-100 m space between the centre of the devices.

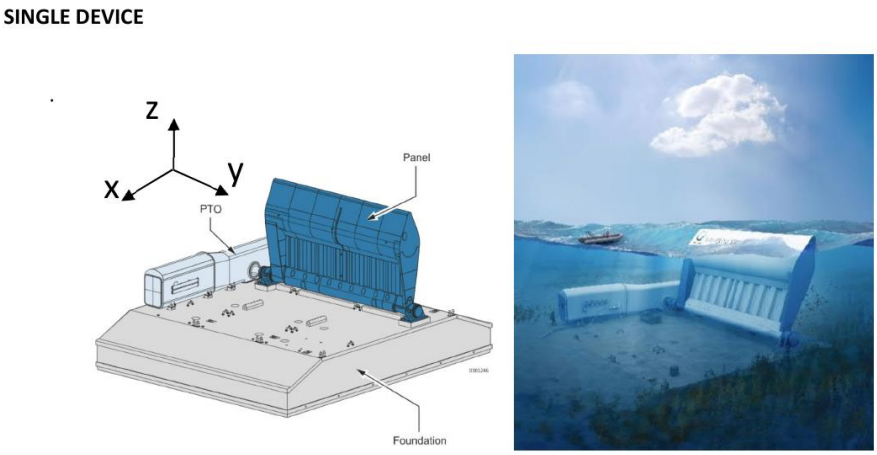

Figure 10: Waveroller energy converter.

4.1.2 Test Site and WEC Array Setup

AW energy has selected Peniche as a test site for the Waveroller device which was installed at Praia da Almagreira in 2020 (Figure 11) approximately 700 meters form the shoreline at 10 meters water depth. Based on the location of this device, an array of 17 WECs, divided into two rows (Figure 12), were created to be included in the simulations.

Figure 11: Testing site location. Bottom image (red circle) shows the location where the WEC is installed.

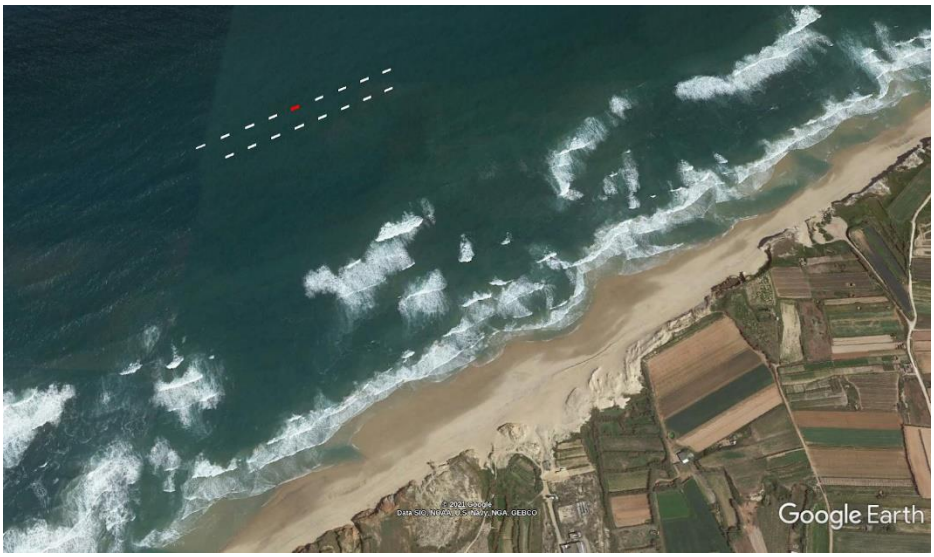

Figure 12: Array of WEC devices used in the simulations. Red line is the location of the Waveroller installed at Praia.

As mentioned previously, WEC devices have their energy absorption efficiency varying with wave frequency and amplitude. According to the Waveroller technical specification the device is efficient at high frequencies (0.3 to 0.2 Hz) decaying significantly toward low frequencies. The range of operation frequencies also do not cover the entire wave energy spectrum. Those characteristics suggests that impact of the WEC array in the coastal wave climate may vary according to the incident wave spectrum.

4.1.3 Dynamic Downscaling

When simulating small scale processes (order of few km) with spectral wave models, boundary conditions containing offshore information are needed. Boundary conditions are commonly sourced from larger scale models (regional or global) and are provided in two distinct forms: Bulk wave parameters (Significant Wave Height, Peak period, wave direction and directional spreading) later used to reconstruct a parametric two-dimensional wave spectrum; the full 2-dimensional wave spectrum.

The first option is used when details of the energy distribution in the directional wave spectrum are less important, however when the opposite occurs, a proper representation the energy distribution in frequency and direction is paramount for a correct assessment. While bulk wave parameters for global and regional models are widely and freely available, the same does not occur for full wave spectrum. For that reason, a dynamic downscaling composed of 4 nested grids have been carried out.

The simulations are based on a combination of three coarser grids running the WaveWachtIII model and a 1 km grid running SWAN (Table 1 and Figure 13). All levels are forced with wind obtained from the Global Forecast System (GFS) produced by the National Centers for Environmental Prediction (NCEP). Simulations were carried out in a non-stationary mode for the year of 2020.

Table 1:Downscalling nested grid structure.

Level	1	2	3	4	5
Model	WWIII	WWIII	WWIII	SWAN	SWAN-SNL
Domain	Global	North Atlantic	Portugal	PT Coast	Peniche
Spatial Resolution	1°	0.25°	0.05°	1 km	40 m
Wind	GFS 25 km GFS 50 km				No
Simulation	1-year non-stationary nested				1-year stationary (3h)

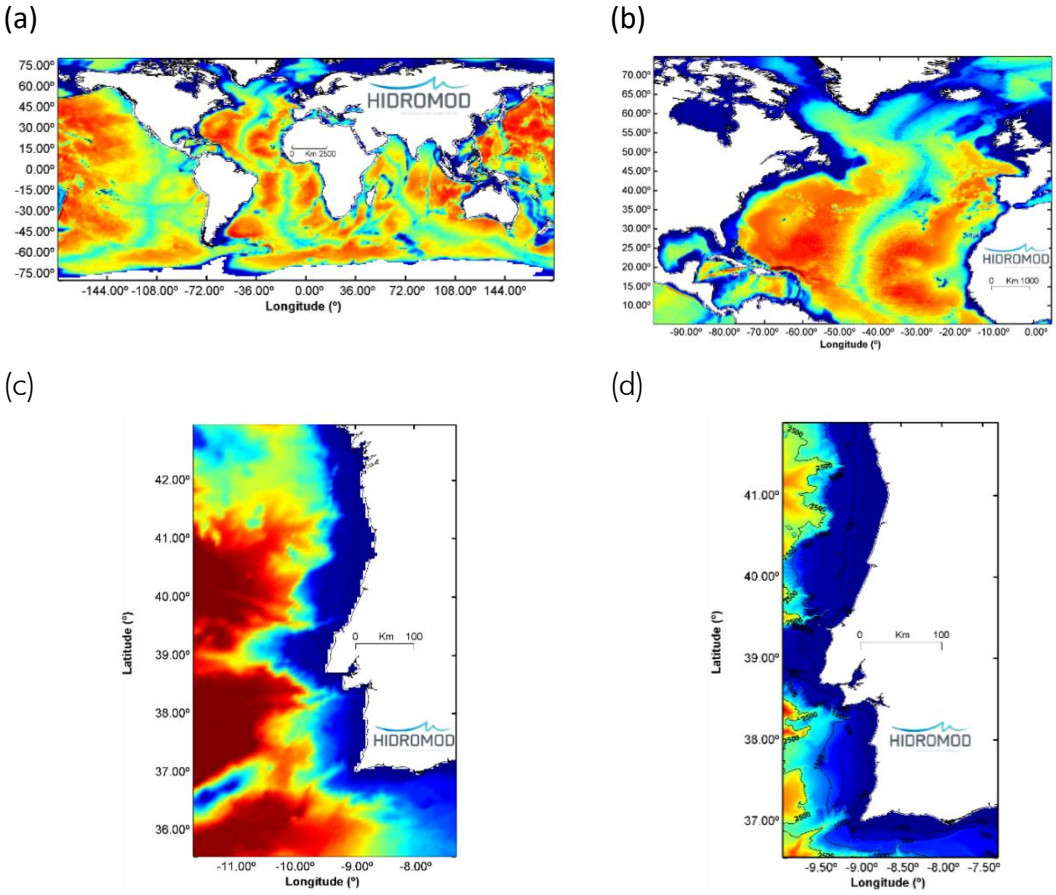

Figure 13: Domain of the 4 nested grid levels use to generate boundary conditions for the SNL-SWAN. Grid levels 1(a), 2(b), 3(c) and 4(d).

The full spectrum provided by the swan grid is then used to force stationary simulations (every 3 hours) for the SWAN-SNL model (Figure 14). Similar to the methodology presented previously, simulations are performed with and without the array of wave energy converters. Results are then analysed in terms of changes in the wave climate associated to the presence of the WEC array. The analysis is presented in terms of changes in both wave bulk parameters and full wave spectrum.

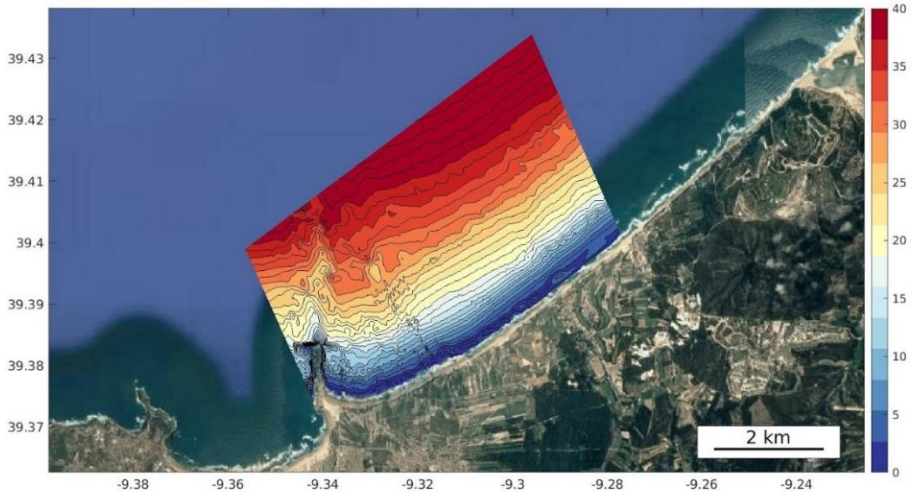

Figure 14: Domain of the Level 5 (SNL-SWAN).

4.2 Morphodynamic Modelling

Morphological evolution is evaluated by calculating initial sediment dynamic tendencies. The simulations are performed with the NearCoM-TVD (Nearshore Community Model) which is a model system for nearshore wave, circulation and sediment processes. NearCOM-TVD couples the nearshore circulation model, SHORECIRC, the wave model SWAN and several sediment transport modules, such as Kobayshi et al. (2008), Soulsby (1997) and van Rijn et al. (2011).

Four simulations have been performed taking as boundary condition the yearly-mean wave climate (S1); summer and winter mean wave climate (S2 and S3, respectively); and an extreme wave condition (S4). The values of Hs and TP used in each scenario are shown in Table 2.

Table 2: Boundary condition for morphodynamic simulations.

Simulation	Hs (m)	Tp (s)
S1	2.0	11
S2	1.3	8.5
S3	2.9	12.5
S4	8.0	18

Results are analysed in terms of changing in sediment deposition between simulations with and without the WEC array.

4.3 Results

4.3.1 Dynamic Downscaling

The simulation configuration presented in section 4.1.3 is part of the forecast system implemented and maintained by Hidromod. The results of the simulations are constantly verified against a series of directional wave buoys deployed along the Portuguese coast that are maintained by the Portuguese Hydrographic Institute (Figure 15).

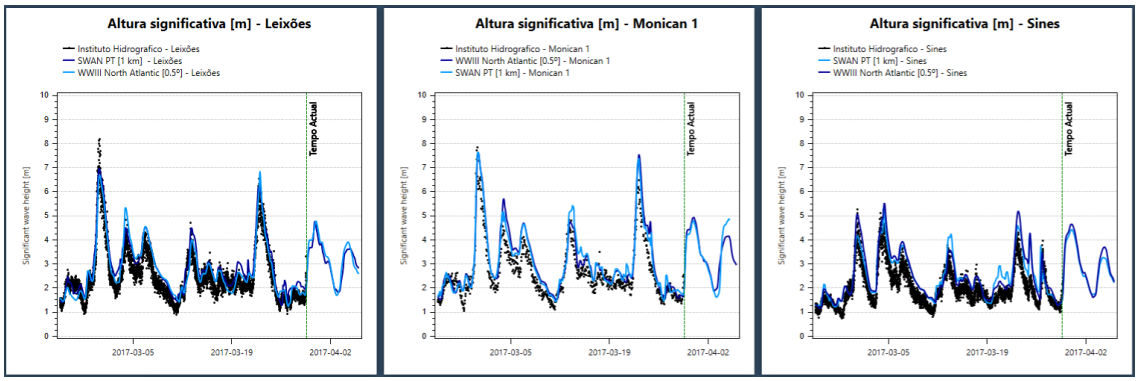

Figure 15: Significant wave height comparison between downscaling modelling system and three directional wave buoys (left – Leixões, middle – Nazaré and right – Sines).

4.3.2 Bulk Wave Parameters

As shown in Figure 16 the effects of the WEC array are stronger close to the lee of the structure (15% on average) reducing towards the shoreline. As shown in Figure 17 the array impact occurs mostly in the outer surf zone and is minimal close to the swash zone.

The results also show that the impact of the WEC array vary depending on the seasonal wave climate. The relative Hs decay is smaller during winter months in comparison with summer months, both in intensity and area (Figure 18). This seasonal pattern occurs mainly due to the period of the incident waves and the frequency dependence efficiency of the WEC. As shown in Figure 19 the peak wave period in the winter months is generally higher than in summer months (Figure 20), and since, the device is more effective for short-period waves.

The results also show that during large storms the array offers little protection to the shoreline. That is a consequence of the type of storms reaching the Portuguese coast with high peak periods that are off the range of operation of the WEC (Figure 19).

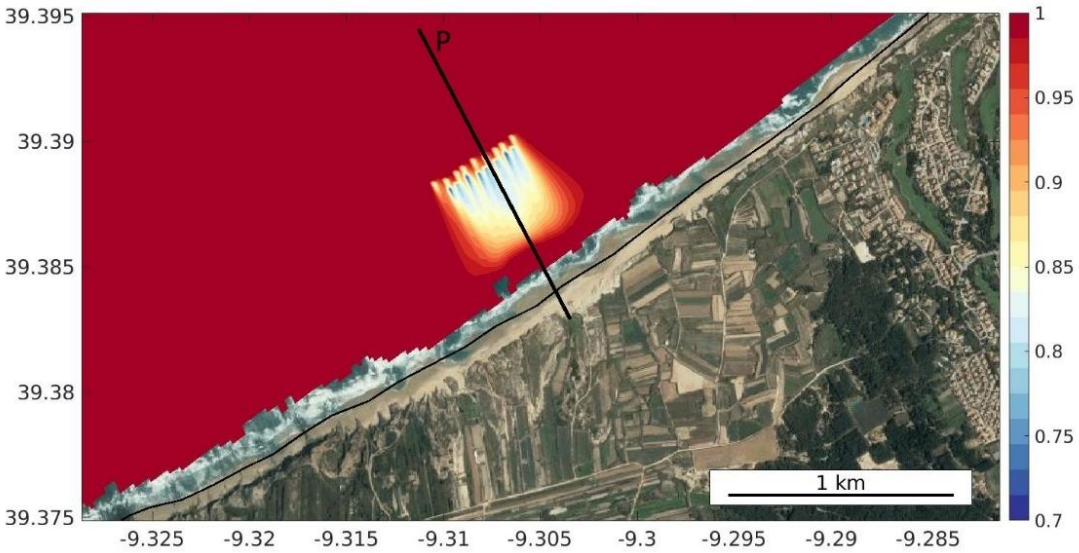

Figure 16:Yearly mean significant wave height ratio (Hs_{WECs}/Hs).

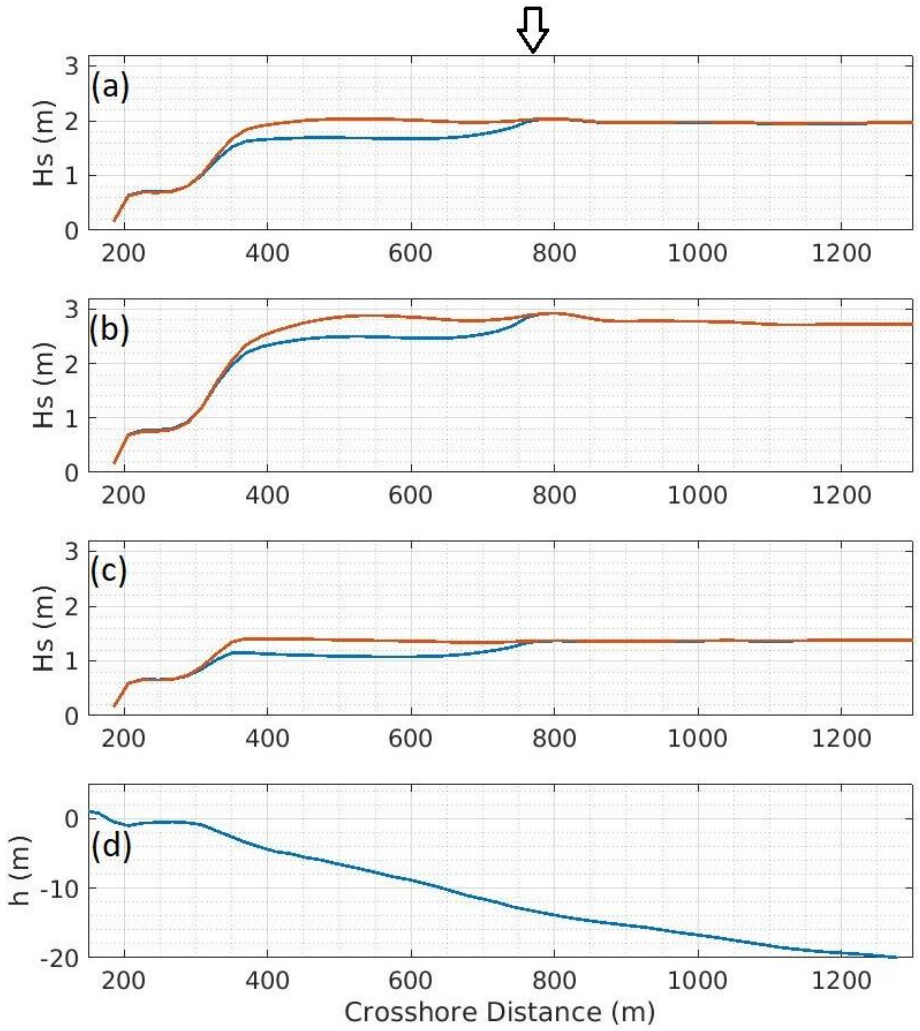

Figure 17:Crosshore evolution of *Hs*, (a) yearly mean, (b) winter-month mean, (c) summer-month mean and (d) depth profile. Blue and red line with and without WEC array, respectively.

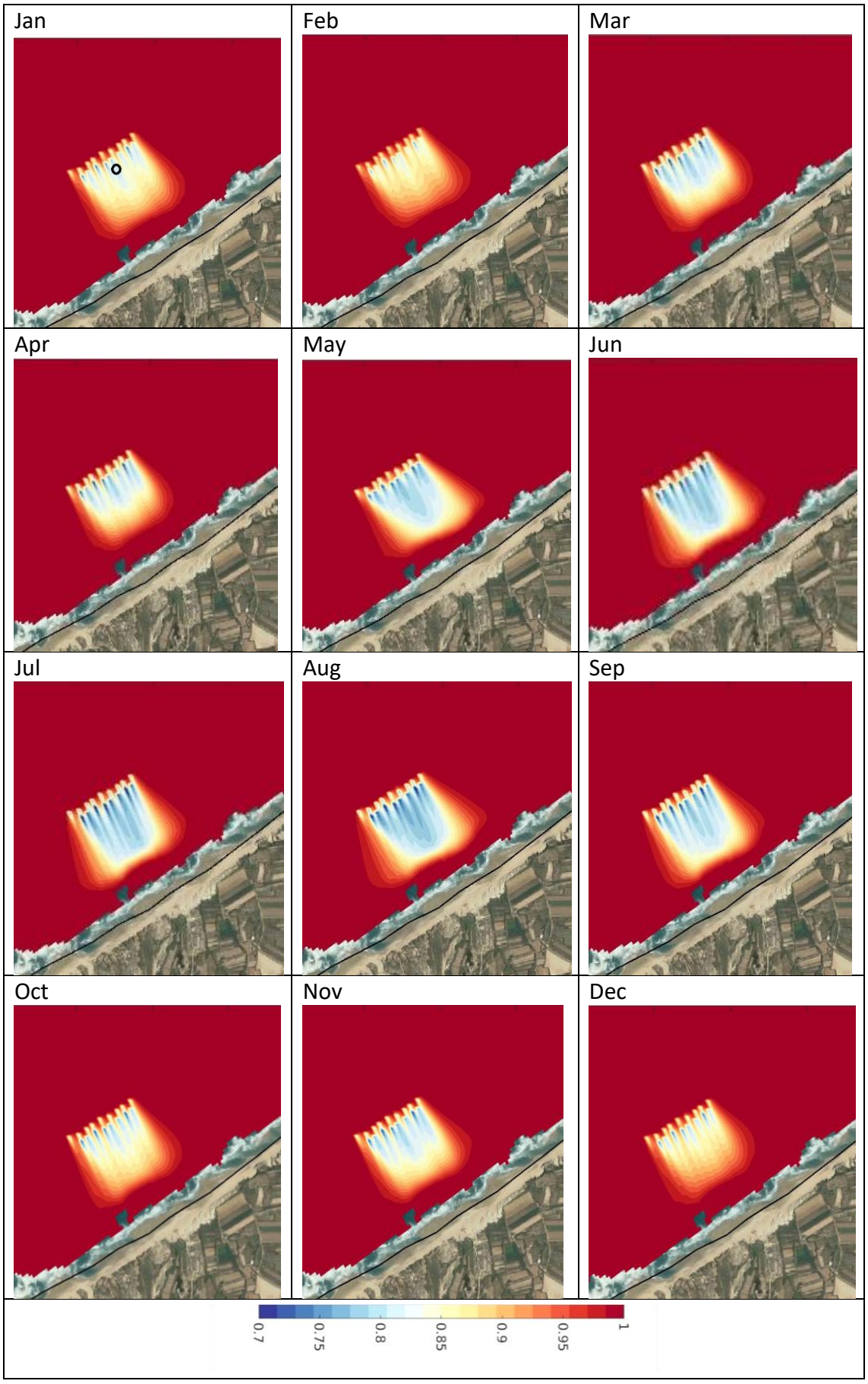

Figure 18: Monthly mean significant wave height ratio (Hs_{WECs}/Hs).

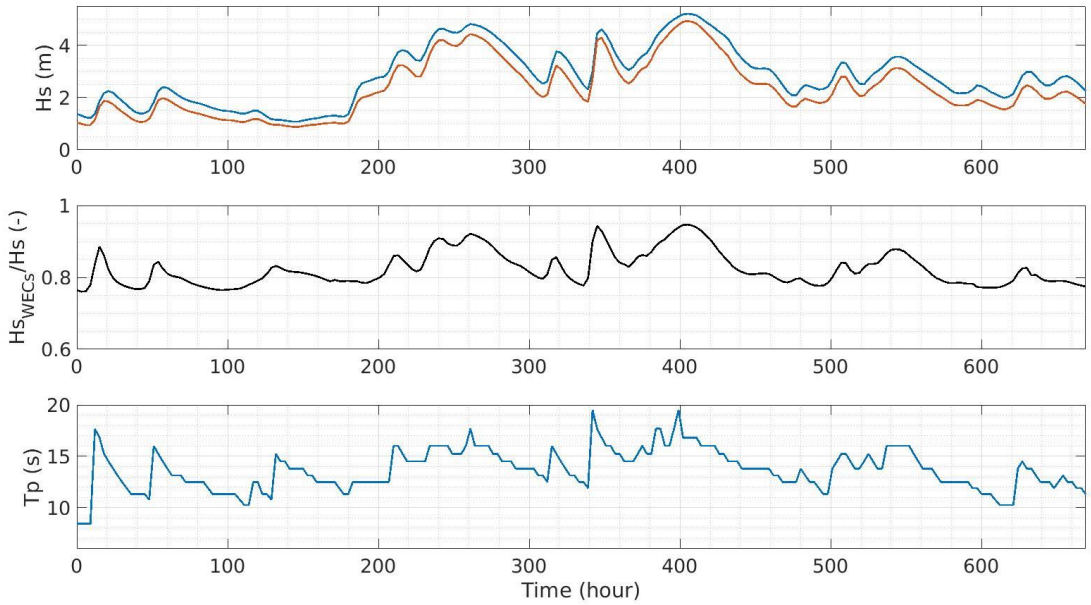

Figure 19: Top panel: monthly (February) evolution of significant wave height, with (red line) and without WEC array (blue). Middle panel: *Hs* ratio. Bottom panel: peak wave period.

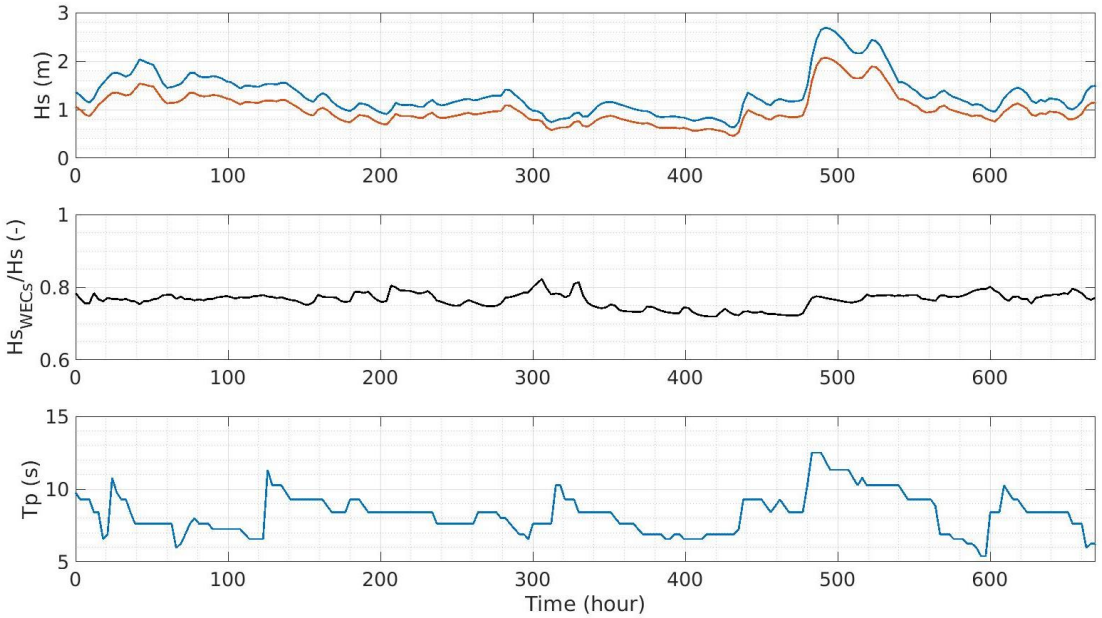

Figure 20: Top panel: monthly (August) evolution of significant wave height, with (red line) and without WEC array (blue). Middle panel: *Hs* ratio. Bottom panel: peak wave period.

4.3.3 Full Wave Spectrum

The frequency dependence efficiency of the WEC results in a variable amount of energy taken from the wave spectrum. The results show that during winter months the energy in the spectrum is located mostly at low frequencies, with a significant part of the energy located outside the WEC's range of operation (Figure 21). This partial removal (in

frequency) of the energy results in changes of shape of the spectrum. As shown in Figure 21 and 22 at the lee of the array the spectrum becomes narrower with a slight change to lower peak frequencies.

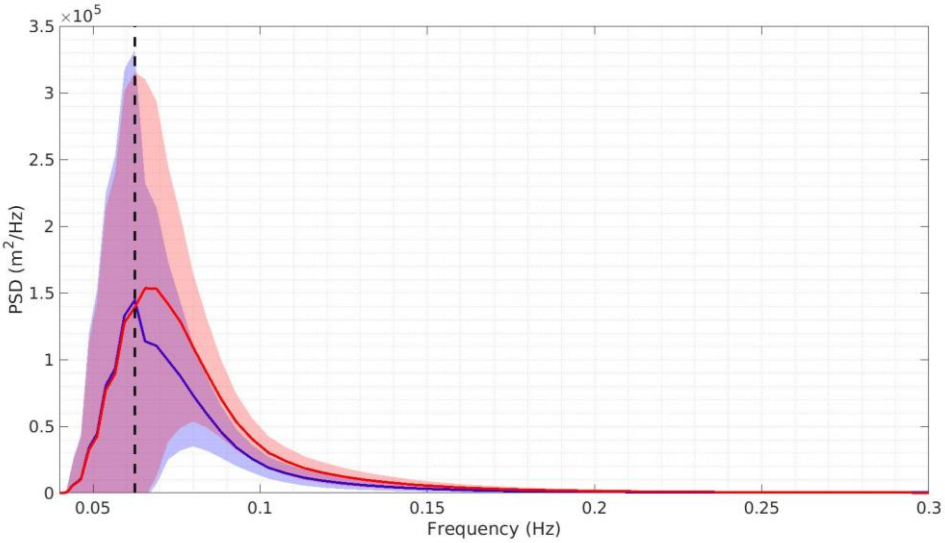

Figure 21: Monthly (February) mean wave spectrum and respective standard deviation (shaded colours). Red line and light red shade simulations without WEC array. Blue line and light blue shade simulations with WEC array.

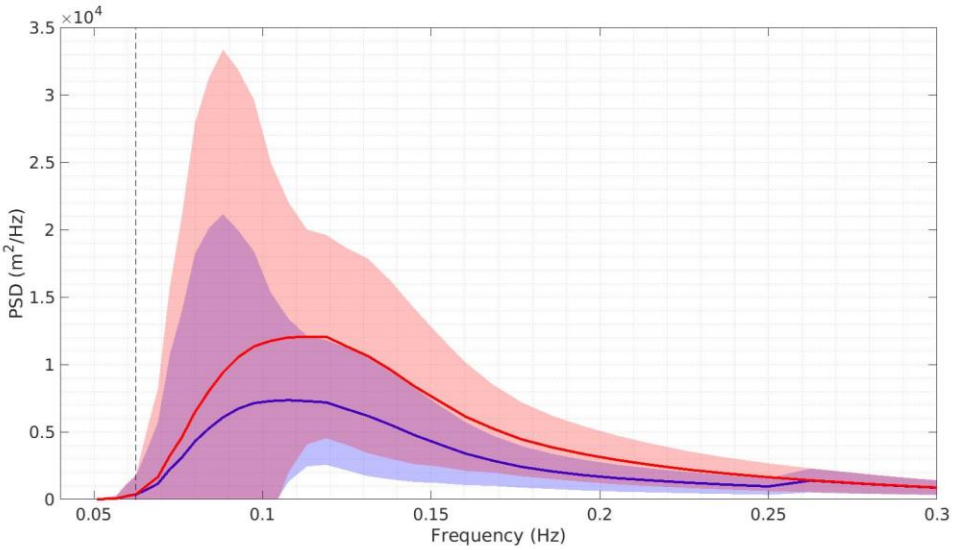

Figure 22: Monthly (August) mean wave spectrum and respective standard deviation (shaded colours). Red line and light red shade simulations without WEC array. Blue line and light blue shade simulations with WEC array.

The effects of the WEC array on wave direction and directional spreading have also been evaluated, and the results show no significant changes in those parameters (Figure 23 and Figure 24). The array is located very close to the surf zone, in shallow waters, where most of the wave refraction has already occurred and the waves are already propagating perpendicular do the shoreline.

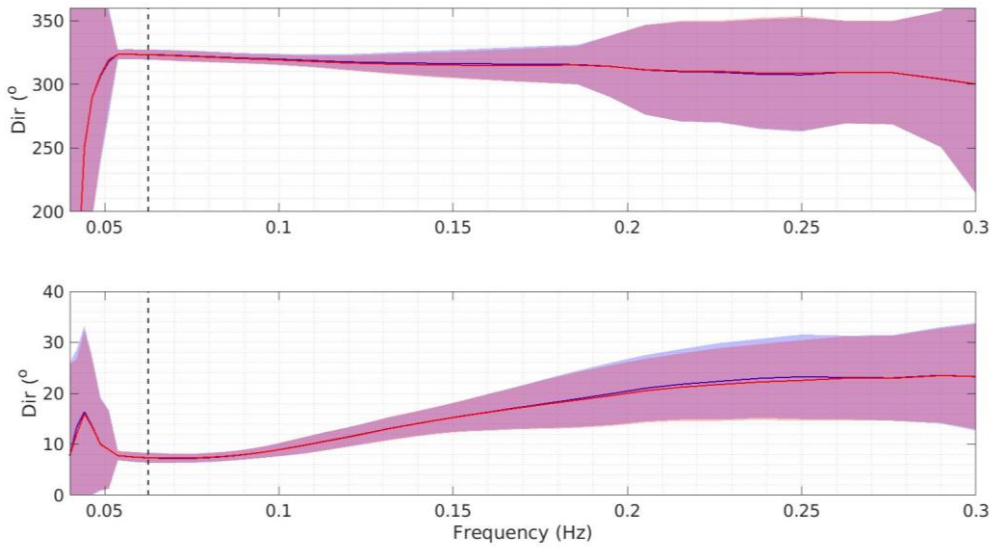

Figure 23: Monthly (February) mean wave direction (top panel) and mean directional spreading (bottom panel), by frequency, and respective standard deviation (shaded colours). Red line and light red shade simulations without WEC array. Blue line and light blue shade simulations with WEC array.

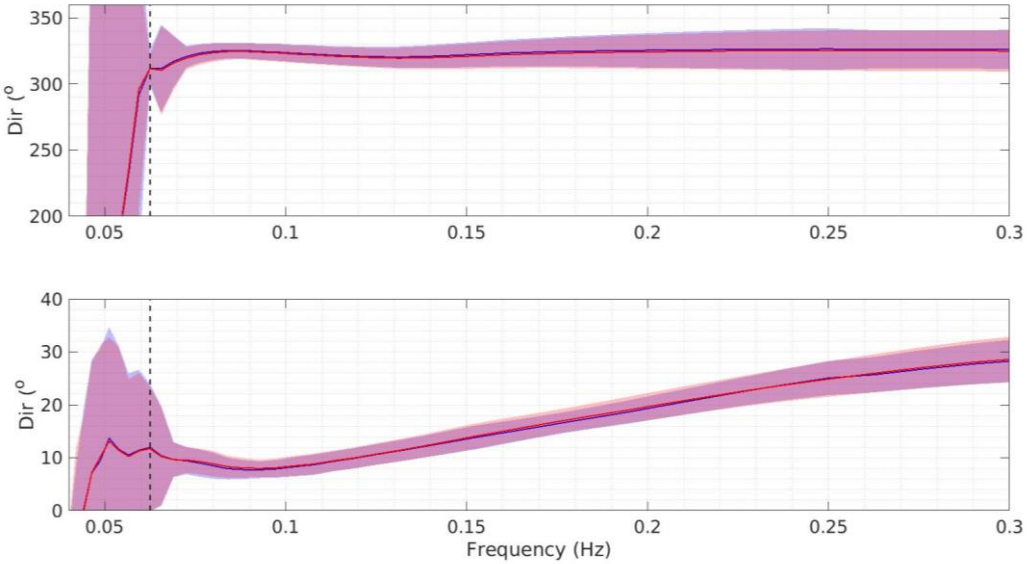

Figure 24: Monthly (August) mean wave direction (top panel) and mean directional spreading (bottom panel), by frequency, and respective standard deviation (shaded colours). Red line and light red shade simulations without WEC array. Blue line and light blue shade simulations with WEC array.

4.3.4 Morphodynamics

The results of morphological evolution simulated with NearCOM-TVD for the 4 scenarios detailed in section 4.2 indicates that most of the changes in the sediment transport (comparing simulations with and without the WEC array) occurs mainly due to small changes in the orientation of the rip-channels and their associated circulation

cells (Figure 25). As expected during the mild wave condition the sediment transport becomes restricted to the very shallow water close to the swash zone.

During extreme conditions, the surf zone extends past the location of the WEC array, and the entire region becomes a saturated surf zone. As indicated previously, due to the characteristics of the WEC during this type of wave condition little energy is removed from the system by the array. As consequence, only small changes in currents and sediment transport are observed (Figure 26).

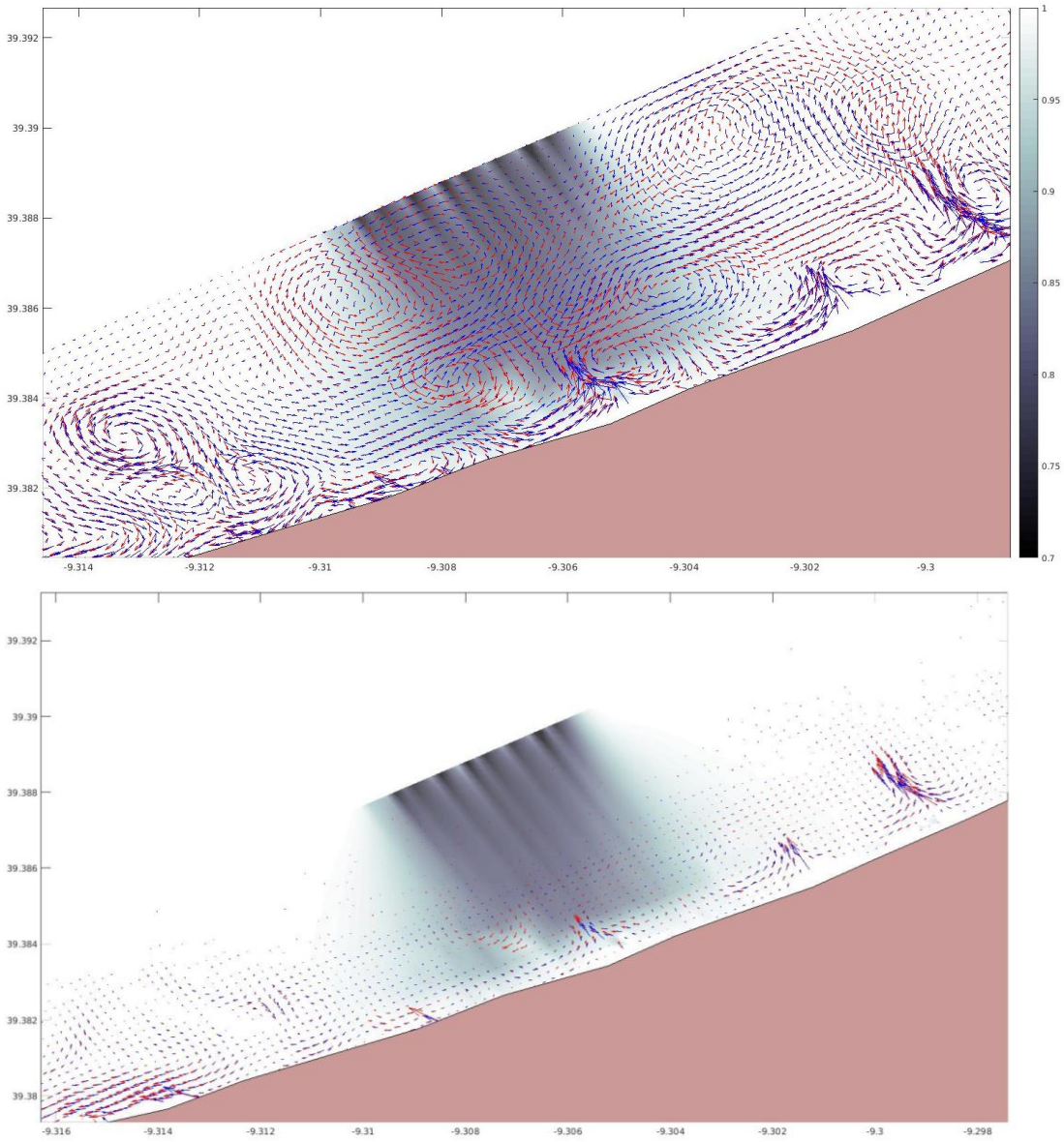

Figure 25: Top panel depth-average current velocity; bottom panel sediment flux for simulation S2 (Summer mean wave climate). Red and blue arrows simulations without and with WEC array, respectively. Gray colormap is the Hs ratio (Hs_{WECs}/Hs).

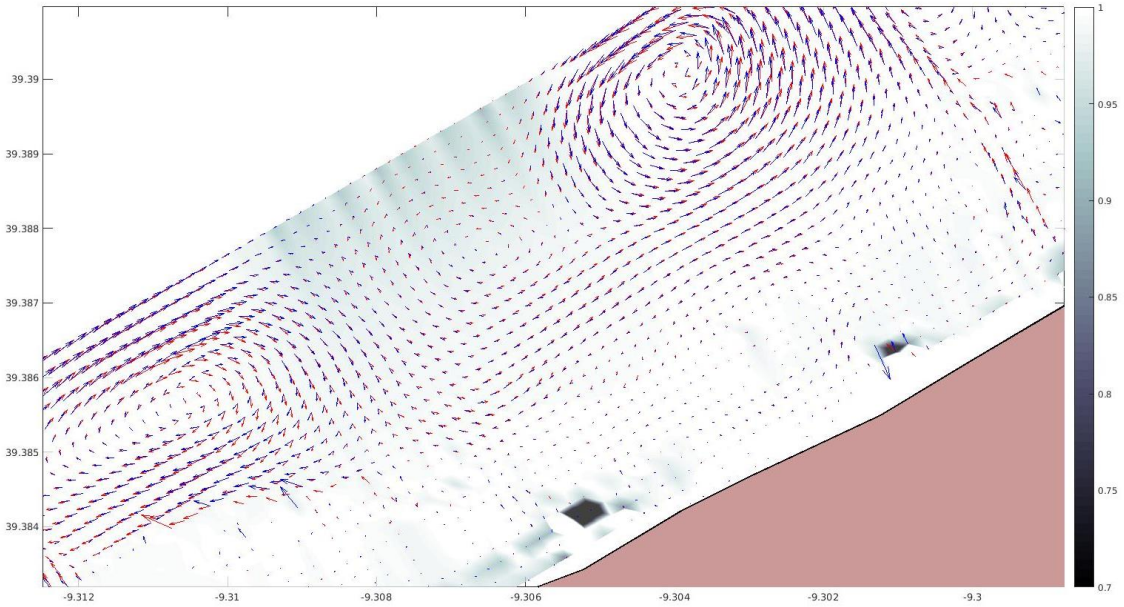

Figure 26: Depth-average current velocity. Red and blue arrows simulations without and with WEC array, respectively. Gray colormap is the Hs ratio (Hs_{WECs}/Hs).

5. Conclusion

In the present study the impact of WEC farms in nearshore morphodynamics is evaluated in two distinct case studies. In the first case the hydrodynamics and beach shoreline evolution is studied by means of a probabilistic approach; and in the second case wave and morphodynamic evolution is analysed using a dynamic downscaling methodology.

In the first case, the WEC farm studied is composed by 80 WECs deployed at 80m water depth at 4km from the coast in the Bimep area.

Five hydrodynamic indicators (*NI, NImax, MNI, RNI, IE*) and two morphodynamic indicators (*y, SI*) are used to analyse the nearshore impact.

The NI_{50} in terms of P and Hs vary in a range of -2000w/m - -4w/m and -0.06m – 0m, respectively and present maximum reduction values (*NImax*) of 41443w/m and 0.45m located in front of a cliff area.

The changes associated with the RNI_{50} ranges from -8% - 0% and -5% - 0% for P and Hs, respectively. Reductions of P and Hs greater than 10% are only recorded during 40% and 4% of the time, respectively.

The impact extension (IE) is of 5.5 km for P and 3 km for Hs and only covers rocky cliff areas.

The P and Hs reduction produced by the WEC farm is limited and with little effect at the coastline. This is attributed to the long distance at which the WEC farm is located from the coastal zone, which is far enough to significantly reduce the wave shadowing effect that occurs in the vicinity of the WEC farm.

The morphodynamic impact is quantified in the only beach of the study site (Bakio beach) where the hydrodynamic impact is limited (NImax of 7000w/m and 0.1m in terms of P and Hs, respectively).

The SI is low (less than 3m) and not homogeneous along the beach. While the western part of the beach undergoes a slight accretion (+2m), the central area is hardly modified, and it is only on the eastern contour of the beach where erosion (-1.5m) occurs. Since, both accretion and erosion magnitudes are considerably low, it could consider that the WEC farm does not provide any protective effect for the beach.

In the second case study, the impact of an array of 17 bottom-mount Waveroller devices were analysed in terms of energy removed from the system by the devices and its impact on the nearshore morphological evolution. A dynamic downscaling

methodology is used to provide full wave spectrum as boundary condition allowing the evaluation of the WEC array impact on nearshore wave spectrum.

Results show that the WEC array not only removes energy from the system but can also change the shape of the transmitted wave spectrum. It has been identified that due to the frequency dependence of the Relative Capture Width curve the effects of the array vary depending on the characteristics of the wave climate. For the typical Portuguese west coast wave climate, the array of WECs tend to work more efficiently during summer periods, where wave spectral energy is located at higher frequencies. Results also indicate that the WEC array offers little protection to extreme wave conditions due to the frequency operation limits of the Waveroller.

The simulated initial sediment transport tendencies show that most of the changes occur in the orientation of rip channels, mostly in the crosshore direction, which is expected due to the nature of the simulations. No significant sediment exchange between long shore areas have been observed. However, it is important to note that additional studies would be necessary to determine long term sediment transport patterns.

6. References

Abanades, J., Greaves, D., Iglesias, G., 2015. Coastal defence using wave farms: The role of farm-to-coast distance. Renew. Energy 75, 572–582.

Abanades, J, Greaves, D., Iglesias, G., 2014a. Coastal defence through wave farms. Coast. Eng. 91, 299–307. https://doi.org/10.1016/j.coastaleng.2014.06.009

Abanades, J, Greaves, D., Iglesias, G., 2014b. Wave farm impact on the beach profile: A case study. Coast. Eng. 86, 36–44. https://doi.org/10.1016/j.coastaleng.2014.01.008

Atan, R., Finnegan, W., Nash, S., Goggins, J., 2019. The effect of arrays of wave energy converters on the nearshore wave climate. Ocean Eng. 172, 373–384.

Bergillos, R.J., Rodriguez-Delgado, C., Allen, J., Iglesias, G., 2019a. Wave energy converter geometry for coastal flooding mitigation. Sci. Total Environ. 668, 1232–1241.

Bergillos, R.J., Rodriguez-Delgado, C., Iglesias, G., 2019b. Wave farm impacts on coastal flooding under sea-level rise: A case study in southern Spain. Sci. Total Environ. 653, 1522–1531.

Birkemeier, W.A., 1985. Field data on seaward limit of profile change. J. Waterw. Port, Coastal, Ocean Eng. 111, 598–602.

Camus, P., Mendez, F.J., Medina, R., Cofiño, A.S., 2011. Analysis of clustering and selection algorithms for the study of multivariate wave climate. Coast. Eng. 58, 453–462. https://doi.org/10.1016/j.coastaleng.2011.02.003

Camus, P., Mendez, F.J., Medina, R., Tomas, A., Izaguirre, C., 2013. High resolution downscaled ocean waves (DOW) reanalysis in coastal areas. Coast. Eng. 72, 56–68.

Carballo, R., Iglesias, G., 2013. Wave farm impact based on realistic wave-WEC interaction. Energy 51, 216–229.

Chang, G., Ruehl, K., Jones, C.A., Roberts, J., Chartrand, C., 2016. Numerical modeling of the effects of wave energy converter characteristics on nearshore wave conditions. Renew. Energy 89, 636–648.

Chen J.-L., Shi F., Hsu T.-J., and Kirby, J. T., 2014, NearCoM-TVD - A quasi-3D nearshore circulation and sediment transport model, Coastal Engineering, 91, 200-212

Contardo, S., Hoeke, R., Hemer, M., Symonds, G., McInnes, K., O'Grady, J., 2018. In situ observations and simulations of coastal wave field transformation by wave energy converters. Coast. Eng. 140, 175–188.

Iglesias, G., Carballo, R., 2014. Wave farm impact: The role of farm-to-coast distance. Renew. Energy 69, 375–385.

Magagna, D., Uihlein, A., 2015. Ocean energy development in Europe: Current status and future perspectives. Int. J. Mar. Energy 11, 84–104.

McNatt, J.C., Porter, A., Chartrand, C., Roberts, J., 2020. The Performance of a Spectral Wave Model at Predicting Wave Farm Impacts. Energies 13, 5728.

Mendoza, E., Silva, R., Zanuttigh, B., Angelelli, E., Andersen, T.L., Martinelli, L., Nørgaard, J.Q.H., Ruol, P., 2014. Beach response to wave energy converter farms acting as coastal defence. Coast. Eng. 87, 97–111.

Millar, D.L., Smith, H.C.M., Reeve, D.E., 2007. Modelling analysis of the sensitivity of shoreline change to a wave farm. Ocean Eng. 34, 884–901.

Putrevu, U. and I. A. Svendsen, 1999, Three-dimensional dispersion of momentum in wave-induced nearshore currents, Eur. J. Mech. B/Fluids, 83-101.

Rusu, E., Soares, C.G., 2013. Coastal impact induced by a Pelamis wave farm operating in the Portuguese nearshore. Renew. Energy 58, 34–49.

Zanopol, A.T., Onea, F., Rusu, E., 2014. Coastal impact assessment of a generic wave farm operating in the Romanian nearshore. Energy 72, 652–670.

Zanuttigh, B., Angelelli, E., 2013. Experimental investigation of floating wave energy converters for coastal protection purpose. Coast. Eng. 80, 148–159.

This project has been funded by the European Commission under the European Maritime and Fisheries Fund (EMFF), Call for Proposals EASME/EMFF/2017/1.2.1.1 – "Environmental monitoring of wave and tidal devices". This communication reflects only the author's view. EASME is not responsible for any use that may be made of the information it contains.

AZTI MEMBER OF BASQUE RESEARCH & TECHNOLOGY ALLIANCE · WavEC Offshore Renewables · IDOM · BiMEP Biscay Marine Energy Platform · CTN · WAVEROLLER® by AW-Energy · HIDROMOD